

of short-term departures from the general trend, analogous to the inset in Fig. 3. With that understanding, the best fitting line has an overall drift of -0.0569° per day, in fair agreement with both the Voyager and HST drifts measured over hundreds of days. The fact that the HST drift is much closer to the longer term mean may be attributable to a fortuitous placement of the two coincident, accurate observations in June 1991 very near the mean position.

Because the value -0.0569° per day refers to a much longer time base line and is therefore less sensitive to temporary departures from the mean, we believe that it determines the best value for the rotation rate of system III so far. The rotation rate of Saturn's system III given by Desch and Kaiser (3) is $810.794^\circ \pm 0.148^\circ$ per day. The revised value, on the basis of this interpretation, is $810.737^\circ \pm 0.008^\circ$ per day.

There is also a short-term motion in the November 1990 images. The line in Fig. 3 that best fits the data from these images gives a rotation rate of $0.96^\circ \pm 0.10^\circ$ per day in the opposite direction to, and much faster than, the long-term drift. This rate implies a velocity of 3.27 ± 0.34 m/s. The time scale of this short-term motion is at least 9 days, and the deviation of the spot from its average value can be as large as 4.3° in longitude or ~ 1250 km. As noted above and by Godfrey (2), there were similar short-term motions in the Voyager data (Fig. 4). Systematic studies of short-term variation in the spot location will be an interesting task for future HST observations. In addition, the HST has the unique capability of verifying the continuous existence of this spot over long time frames.

Allison *et al.* (10) treated the hexagon as a planetary wave stimulated by the associated spot. In this study, we have shown that the spot and hexagon are both long-lived features of Saturn; since they were discovered, we have not seen one without the other. The long-term movement of the spot is also closely related to Saturn's internal rotation. Observations of this relation are consistent with the spot's being deeply rooted in Saturn's interior, acting as a stimulus in the polar jet and creating a wave structure visualized as the polar hexagon. We look forward to HST observations between 1996 and 2010 to see if the southern hemisphere has a structure and stability similar to that of the northern hexagon and spot.

REFERENCES AND NOTES

1. D. A. Godfrey, *Icarus* 76, 335 (1988).
2. ———, *Science* 247, 1206 (1990).
3. M. D. Desch and M. L. Kaiser, *Geophys. Res. Lett.* 8, 253 (1981).
4. J. A. Westphal *et al.*, *Icarus* 100, 485 (1992).
5. J. A. Westphal *et al.*, *Astrophys. J.* 369, L51 (1991).

6. T. R. Lauer, *Publ. Astron. Soc. Pac.* 101, 445 (1989).
7. C. C. Cunningham and D. M. Anthony, *Icarus*, in press.
8. L. B. Lucy, *Astron. J.* 79, 745 (1974).
9. The transformation from the coordinates in polar projection (x_p, y_p) to the corresponding coordinates in γ -projection (x', y') is given by

$$\begin{aligned} x' &= x_p \cos \gamma - \frac{b}{a} \sqrt{a^2 - r_p^2} \sin \gamma \\ y' &= y_p \end{aligned} \tag{1}$$

where $r_p = \sqrt{x_p^2 + y_p^2}$ is the distance of the point from the pole in polar projection and γ is the angle between the line of sight and the south-north axis of the planet. One obvious restriction on (x_p, y_p) for the transformation is $r_p \leq a$. Another restriction is

$$\frac{x_p}{\sqrt{a^2 - r_p^2}} \geq -\frac{a}{b \tan \gamma} \tag{2}$$

Otherwise, the point (x_p, y_p) is not visible in the

γ -projection. To determine the planetocentric latitude and longitude of the spot from the polar-projected image, we used

$$\tan \theta = \frac{a}{b} \frac{r_p}{\sqrt{a^2 - r_p^2}} \quad \cos \phi = \frac{x_p}{r_p} \tag{3}$$

where θ is measured from the north pole and ϕ is measured from the central meridian.

10. M. Allison, D. A. Godfrey, R. F. Beebe, *Science* 247, 1061 (1990).
11. We acknowledge the National Space Science Data Center (NSSDC) and the imaging-team leader from the Voyager project, B. A. Smith, for providing the Voyager images used in this analysis. C.D.B. thanks the National Academy of Sciences-National Research Council associateship program for providing the opportunity to process these data while at the NASA Goddard Space Flight Center.

15 September 1992; accepted 19 January 1993

Ground-Based Observations of Saturn's North Polar Spot and Hexagon

A. Sanchez-Lavega, J. Lecacheux, F. Colas, P. Laques

Ground-based observations of two conspicuous features near the north pole of Saturn, the polar vortex and the hexagonal wave structure, were made from July 1990 to October 1991, 10 years after their discovery. During this period the polar spot drifted in longitude, relative to system III, by -0.0353° per day on average. Superimposed on this mean motion, the spot also underwent short-term rapid excursions in longitude of up to $\sim 14^\circ$ at rates of up to $\sim 1^\circ$ per day. The spot also exhibited irregular variations in its latitude location. A combination of these data together with those obtained by Voyager 1 and 2 in 1980 and 1981 shows that the spot drifted -0.0577° per day for the 11-year interval from 1980 to 1991. The large lifetime of both features indicates that they are insensitive to the strong variations in the seasonal heating of the cloud layers in the upper polar atmosphere.

Voyager images of Saturn obtained in 1980 and 1981 revealed the presence of a hexagonal cloud structure located at planetographic latitude 78.7°N encircling the north pole (1). Associated with it, an oval spot, nicknamed Big Bertha by the Voyager imaging team (2), was observed impinging on the southern flank of one of the hexagon edges at 75.9°N . Both features were nearly stationary with respect to the planet's internal rotation (3). We present here ground-based observations of both features 10 years after their discovery and discuss the implications for their motions and structure. We used the 1.05-m-diameter telescope at Pic-du-Midi Observatory to make the measurements. The telescope was equipped with a charge-coupled device (CCD) camera and a

large set of filters covering the spectral range from 0.4 to 1 μm , including narrow-band interference filters centered in the methane absorption bands at 0.619, 0.725, and 0.899 μm (4). Although Saturn had a low declination and altitude above the horizon during the observing period, the usual excellent atmospheric conditions at Pic-du-Midi Observatory and the tilt of the planet as seen from the Earth (20° to 23°) allowed us to observe the polar features from July 1990 to December 1991. Data were available for 23 nights covering a period of 469 days.

Our first observation of the polar spot was made on 4 July 1990 (5). These images also revealed the hexagon, as shown in Fig. 1. The hexagon had been detected on a set of images obtained on 29 June 1989, although the polar spot was not visible because it was on the rear hemisphere. We performed measurements on the latitude and longitude location of the spot center and edges on different sets of frames obtained each night (6). The main source of error arises from the determination of the planet limbs and from the position of the spot itself. We estimate that the average errors are $\sim 2^\circ$ in latitude

A. Sanchez-Lavega, Departamento Fisica Aplicada I, Escuela Técnica Superior de Ingenieros Industriales y de Telecomunicación, Universidad del País Vasco, Alda. Urquijo s/n, 48013 Bilbao, Spain.
 J. Lecacheux, Département de Recherches Spatiales, Observatoire Paris-Meudon, 92190 Meudon, France.
 F. Colas, Bureau des Longitudes, 77 Avenue Denfert Rochereau, 75014 Paris, France.
 P. Laques, Observatoire Pic-du-Midi, 65200 Bagneres-de-Bigorre, France.

and $\sim 4^\circ$ in longitude. The errors increase appreciably as the spot moves away from the central meridian, and so we restricted the measurements to those images in which the spot was within 35° of the central meridian. In these cases the errors remained approximately constant within the above values (Table 1).

The longitude and latitude of the spot's center varied from July 1990 to October 1991 (Fig. 2 and Table 1). A linear least squares fit for the longitude data gives a mean drift of the spot relative to system III of $\omega = -0.0353^\circ \pm 0.005^\circ$ per day. The mean latitude of the spot during this period was $75.8^\circ \pm 1.9^\circ\text{N}$, and thus this drift corresponds to a slow eastward zonal velocity of 0.12 m/s. Several excursions are clearly evident and cannot be attributed to measurement uncertainties. Such excursions are also suggested by the Voyager images (3).

The spot underwent rapid longitude changes relative to the mean motion with maxima of $\sim 14^\circ$ and zonal velocities of up to ~ 4 m/s. No periodic behavior was evident. This irregular motion appears to be confined between the corners of one of the hexagon edges, as shown in Fig. 2. Although it was difficult to measure the position of the hexagon corners because they were not sharp in our images, the data for days 213 (31 July 1990) and 230 (17 August 1990) illustrate clearly that the spot center fluctuated relative to the corners. Because the zonal (east-west) dimension of the spot was $24.2^\circ \pm 3.65^\circ$ (which corresponds to a size of 7000 ± 1000 km), the observed longitude excursions correspond roughly to the distance the spot can move away from the center of the hexagon edge to its corners.

Moreover, the apparent variations in latitude appear to be independent of those

in longitude (Fig. 2) (7). The spot moved irregularly within $\sim 74^\circ\text{N}$ and 80°N without a marked change in its zonal velocity [as could be expected from the zonal wind profile at these latitudes (1)]. A simple explanation is that the hexagon and the eastward jet at 78°N also shifted together with the spot in the meridional direction. However, this would be contrary to the established persistence of the winds of Jupiter (and probably those of Saturn), in both latitude and time. Another possibility is that short-term, local variations in reflectivity within the spot, such as could be produced by the entrainment of small bright clouds along the periphery of the vortex, could cause the center of brightness to shift in latitude.

In order to study the long-term motion of the spot, we combined our data with those obtained 10 years earlier by Godfrey using Voyager images (3). He obtained a mean drift $\omega = -0.040^\circ$ per day for an interval of 282 days during 1980 to 1981, which is close to our value. For the 11-year interval, the average drift is $\omega = -0.0577^\circ$ per day. Differences between these short and long temporal drifts rates could arise simply from the fluctuations described previously or from unobserved oscillations confined between the average drifts indicated in Fig. 3.

Another possibility is that the polar spot observed in the Voyager images and that observed since 1990 are not the same feature. As seen in Fig. 3, the drift lines are separated by $\sim 60^\circ$ (hexagon edge size). This relation suggests that there could be two spots, each one in a contiguous hexagon edge, and that a differential change in their brightness has rendered them visible at different times. Long-term, systematic measurements of the feature are needed to

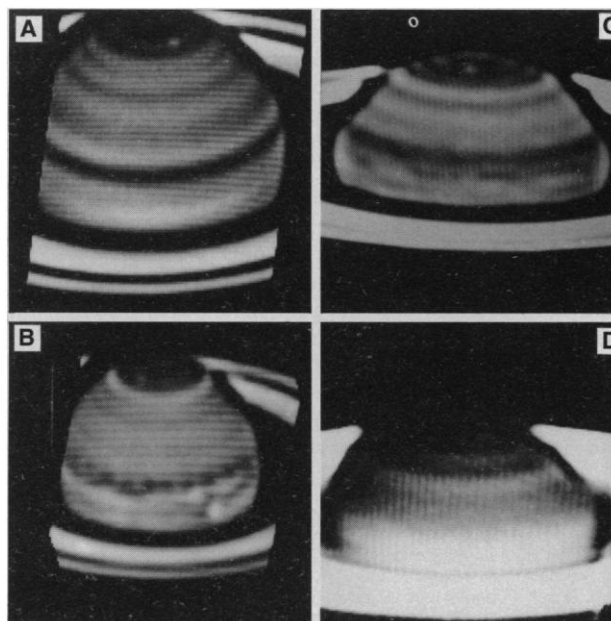
evaluate this possibility. In any case, the rotation period of the polar spot, 10 hours 39 min $22 \text{ s} \pm 1 \text{ s}$, is well within the error indicated by the radio rotation period (6) and could be close to the true saturnian internal rotation period as suggested by Godfrey (3).

Images of the spot taken through a set of filters (4) indicate that, although visible at yellow to red wavelengths, the best contrast and definition are achieved through use of a broadband near-infrared filter I that covers the spectral domain from ~ 0.7 to $1 \mu\text{m}$. The spot is particularly bright under the methane band filters (0.725 and $0.899 \mu\text{m}$) (Fig. 1), but its reflectivity decreases in the nearby continuum wavelengths at 0.750 and $0.830 \mu\text{m}$. The spot was also easily detected under the methane band filters throughout the latitude circle, even when close to the limb. This spectral behavior denotes that the cloud tops of the vortex extend vertically to a particular high altitude. Using the absorption coefficient of the $0.899\text{-}\mu\text{m}$ band (8) convolved with our filter transmission curve and taking account of the local acceleration of gravity in the polar region of $g = 896 \text{ cm/s}^2$ (9) and a saturnian methane abundance of 0.43% by volume (10), we calculate that the unit optical depth is reached at a pressure of 90 ± 10 mbar. A similar conclusion that the vortex clouds were high was obtained from the spectral reflectivity variations observed in Voyager images acquired through violet to orange filters (1, 11).

Table 1. Variation in time (t_o) of the planetographic latitude (ϕ_g) and system III west longitudes (λ_{III}) of the polar spot; t_o is the time in days since 1 January 1990 (0 hours universal time).

| Date | t_o (days) | ϕ_g ($^\circ\text{N}$) | λ_{III} (deg) |
|----------|-----------------|----------------------------------|--------------------------|
| 7/4/90 | 185.99 | $76.4 \pm 2.7^\circ$ | $122.3 \pm 6.2^\circ$ |
| 7/8/90 | 189.0 | 75.9 ± 1.8 | 125.7 ± 1.1 |
| 7/11/90 | 192.15 | 76.1 ± 2 | 123.9 ± 5 |
| 7/12/90 | 193.00 | 76.6 ± 2 | 129.6 ± 5 |
| 7/31/90 | 212.98 | 73.4 ± 0.8 | 118.6 ± 2.1 |
| 8/17/90 | 229.93 | 75.1 ± 1.95 | 142.7 ± 2.7 |
| 9/27/90 | 270.78 | 74.0 ± 2 | 125.3 ± 5 |
| 11/5/90 | 309.76 | 76.6 ± 1.6 | 127.3 ± 7.1 |
| 11/6/90 | 310.73 | 75.2 ± 2 | 124.4 ± 5 |
| 11/14/90 | 318.77 | 75.7 ± 2 | 128.9 ± 5 |
| 11/18/90 | 322.75 | 73.7 ± 2 | 138.6 ± 5 |
| 12/4/90 | 338.71 | 74.2 ± 2 | 125.0 ± 5 |
| 2/24/91 | 420.28 | 73.3 ± 2 | 120.8 ± 5 |
| 6/8/91 | 525.12 | 73.3 ± 2 | 107.3 ± 5 |
| 7/6/91 | 553.13 | 77.0 ± 1 | 122.2 ± 2.5 |
| 7/10/91 | 557.10 | 75.9 ± 1.4 | 114.6 ± 3 |
| 7/12/91 | 558.96 | 77.3 ± 0.3 | 111.0 ± 5 |
| 7/14/91 | 561.1 | 78.6 ± 2 | 114.3 ± 5 |
| 7/15/91 | 562.03 | 80.4 ± 1.7 | 114.9 ± 5 |
| 8/24/91 | 601.95 | 79.7 ± 2 | 118.0 ± 5 |
| 8/25/91 | 602.88 | 76.3 ± 2 | 115.0 ± 5 |
| 9/18/91 | 626.86 | 75.8 ± 0.6 | 115.5 ± 2.5 |
| 10/16/91 | 654.8 | 74.1 ± 0.6 | 111.8 ± 1.2 |

Fig. 1. Processed images of Saturn obtained at Pic-du-Midi Observatory: (A) 17 August 1990, filter I; (B) 5 November 1990, filter I; (C) 10 July 1991, filter I; (D) 18 September 1991, methane absorption band filter at $0.899 \mu\text{m}$. Images (A) and (B) show the hexagon; the polar spot is visible in all four images.



In the Voyager images the greatest contrast was obtained with the use of a violet filter at $0.419 \mu\text{m}$, whereas the spot was barely detected through a green filter at $0.566 \mu\text{m}$ (1). This behavior is contrary to what we observed in 1990 and 1991. This difference may indicate that the cloud properties of the vortex changed during this time interval. The north polar region of Saturn shows a marked color dependence, as seen in our multispectral images and in those obtained with the Hubble Space Telescope (12). This dependence of reflectivity on wavelength reflects the particular vertical distribution of the clouds at the pole, which show significant differences relative to those at temperate and equatorial regions (13, 14). The disposition of the polar cloud cover, together with the existence of the singular hexagon and vortex,

could be a manifestation of a polar atmospheric circulation that deserves further theoretical examination.

Both the polar vortex and the hexagon, if they are the same features as observed by Voyager, are the longest lived cloud features observed so far in Saturn's atmosphere with a lifetime of more than 10 years (15). Measurements at several wavelengths performed on archived photographs since 1922 indicate that a north polar belt has persisted between $\sim 74^\circ\text{N}$ and 80°N (9, 16). Although not resolved in its geometry, this belt could be the hexagon because it occupies the same latitude. If so, the hexagon might have persisted for at least ~ 70 years. A symmetrical long-lived south polar belt was regularly observed in the southern hemisphere from 1880 to 1981 between $74.5^\circ \pm 1.4^\circ\text{S}$ and $81.4^\circ \pm 1.2^\circ\text{S}$ (9, 16).

This belt might also be a wave whose geometrical shape and phase speed would depend on whether a forcing vortex and a sharp zonal jet are present, as suggested by a theoretical model (17). Imaging of the south polar region with ground-based telescopes equipped with CCD cameras and with the Hubble Space Telescope in coming years (when the tilt of the planet as seen from the Earth makes visible the south pole), could lead to the discovery of other such features.

The large lifetime of cloud features poleward of $\sim 74^\circ\text{N}$ seems amazing in view of the strong seasonal insolation cycle at these latitudes (18). For instance, during the period between the Voyager and the Pic observations, the insolation at the top of the atmosphere changed at 80°N from complete darkness in 1979 to a maximum of 5.6 cal/cm^2 per day in 1987; it will decrease again to zero around 1997. Long-term infrared measurements at thermal wavelengths of the north and south polar regions (19) have shown that the temperature changes in accordance with pure seasonal radiative models of the upper troposphere (pressure < 0.6 bar) and stratosphere (20). The persistence of the polar spot and hexagon in spite of the pronounced insolation changes, together with the high-altitude location of their cloud tops, could be an indication that both features extend into the troposphere and that they are not controlled by insolation-radiative processes. Moreover, because they are nearly stationary relative to the radio rotation period, the hexagon and polar spot might originate in the deep interior, as has been recently proposed for some slowly moving features observed in the atmosphere of Jupiter (21). Another possibility, favored by the wave dynamical model (17), is that the large eddy lies in a deep-rooted wind field, insensitive to the seasonal heating, that supports strong anticyclonic circulation at the spot latitude, whereas the hexagon could be a high-altitude wave pattern forced by the vortex.

Fig. 2. Time dependence of the west longitude (system III) (A) and planetographic latitude (B) of the polar spot during the period from July 1990 to October 1991 as measured on Pic-du-Midi images. Day 0 is 1 January 1990 (0 hours universal time); dots are the polar spot; triangles are the hexagon edge corners. The continuous line in (A) is a least square fit to the data; the dashed line in (B) is a mean latitude value.

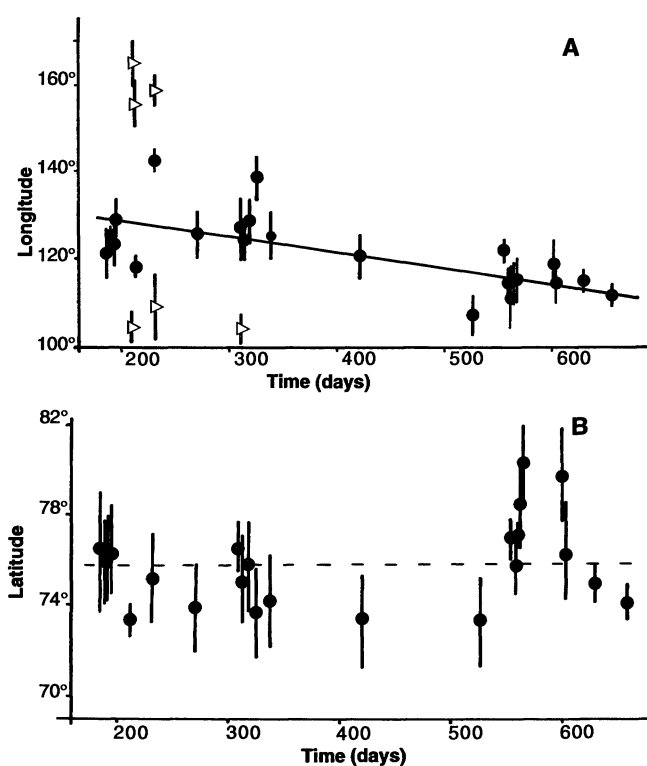
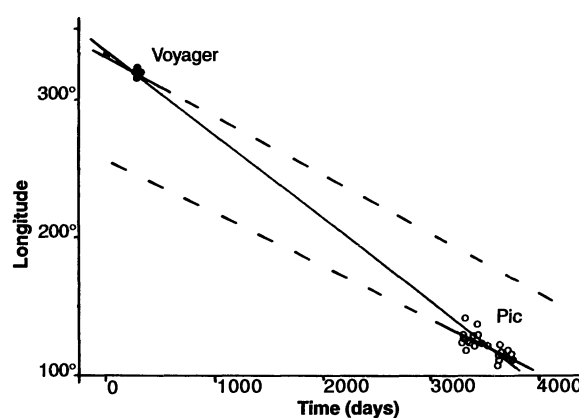


Fig. 3. Time dependence of the longitude of the polar spot during the interval from November 1980 to October 1991 after combining Voyager and Pic-du-Midi measurements. Day 0 is 12 November 1980. The heavy continuous line is the least squares fit to the whole data set. Partial fits to the Voyager and Pic-du-Midi data are indicated by short continuous lines prolonged for the whole interval with dashed lines.



REFERENCES AND NOTES

1. D. A. Godfrey, *Icarus* 76, 335 (1988).
2. B. A. Smith *et al.*, *Science* 212, 163 (1981).
3. D. A. Godfrey, *ibid.* 247, 1206 (1990).
4. See table 1 in A. Sanchez-Lavega *et al.* [*Nature* 353, 397 (1991)] for filter characteristics. Most observations presented in this paper were performed with a Thomson CCD with a pixel size of 0.34 arc sec or 0.14 arc sec depending on whether a Barlow lens was or was not used. With mediocre observation conditions we use exposure times of 0.5 to 1 s (broadband filter I), but under excellent atmospheric conditions we can use exposure times of 5 to 10 s without degrading the image quality. After an image selection and dark-noise and flat-field correction, a lot of ~ 5 - to 10-s frames are recentered with an accuracy of 0.5 pixel and added together. This improves the signal to noise ratio by a factor of ~ 2 to 3, preserving the original resolution. The final image processing includes a contrast enhancement by a

- numeric "unsharp masking," similar in its fundamentals to the well-known photographic technique.
5. F. Colas, J. Lecacheux, P. Laques, R. Despiau, *Int. Astron. Union Circ.* 5052 (1990).
 6. We used system III west longitudes defined relative to a radio rotation period of 10 hours 39 min 24 s \pm 7 s [M. D. Desch and M. L. Kaiser, *Geophys. Res. Lett.* 8, 253 (1981)] and planetographic latitudes defined in (17).
 7. This is contrary to, for example, recent observations of some spots on Neptune [L. A. Sromovsky, *Science* 254, 684 (1991)]. Zonal oscillations have also been reported for some Jupiter spots, such as the Great Red Spot [see B. A. Smith and G. E. Hunt, in *Jupiter*, T. Gehrels, Ed. (Univ. of Arizona Press, Tucson, 1976), pp. 564–585], and at least for a Saturn spot (15).
 8. U. Fink, D. C. Benner, K. A. Dick, *J. Quant. Spectrosc. Radiat. Transfer* 18, 447 (1977).
 9. G. F. Lindal, D. N. Sweetnam, V. R. Eshleman, *Astron. J.* 90, 1136 (1985).
 10. R. Courtin, D. Gautier, A. Marten, B. Bezard, R. A. Hanel, *Astrophys. J.* 287, 899 (1984).
 11. A high-resolution color image of the vortex was published in *Sky Telescope* 62, 430 (1981). In it, it is possible to appreciate the apparent anticyclonic circulation with spiral patterns and a white central core; see also (1) for a full account of streamline patterns.
 12. J. A. Westphall *et al.*, *Astrophys. J.* 369, L51 (1991).
 13. R. A. West *et al.*, *J. Geophys. Res.* 88, 8679 (1983); M. G. Tomasko, R. A. West, G. S. Orton, V. G. Teffell, in *Saturn*, T. Gehrels and M. S. Matthews, Eds. (Univ. of Arizona Press, Tucson, 1984), pp. 150–194.
 14. E. Karkoschka and M. G. Tomasko, *Icarus* 97, 161 (1992). Their study indicates that the ammonia cloud cover expected from phase equilibria will have its base at \sim 1.4 bar and will be absent in the north polar region, where the cloud deck sites are below the 2.5-bar level.
 15. E. J. Reese, *Icarus* 15, 466 (1971). The previous lifetime record for an isolated spot was that observed at 57°S, which lasted about 490 days.
 16. A. Sanchez-Lavega and E. Battaner, *Astron. Astrophys. Suppl. Ser.* 64, 287 (1986); A. Sanchez-Lavega and J. A. Quesada, *Planet. Space Sci.* 36, 1381 (1988).
 17. M. Allison, D. A. Godfrey, R. F. Beebe, *Science* 247, 1061 (1990). Their model interprets the hexagon as a stationary Rossby wave forced by the polar vortex.
 18. A. W. Brinckman and J. Mc Gregor, *Icarus* 38, 479 (1979); R. M. Suggs, thesis, New Mexico State University, Las Cruces (1983); E. Van Helmerijck, *Earth Moon Planets* 38, 217 (1987).
 19. A. T. Tokunaga, J. Caldwell, F. C. Guillet, I. G. Nolt, *Icarus* 36, 216 (1978); *ibid.*, p. 46; B. J. Conrath and J. A. Pirraglia, *ibid.* 53, 286 (1983); D. Y. Gezari *et al.*, *Nature* 342, 777 (1989).
 20. B. E. Carlson, J. Caldwell, R. D. Cess, *J. Atmos. Sci.* 37, 1883 (1980); B. Bezard, D. Gautier, B. Conrath, *Icarus* 60, 274 (1984); B. Bezard and D. Gautier, *ibid.* 61, 296 (1985).
 21. D. Deming *et al.*, *Astrophys. J.* 343, 456 (1989); J. A. Magalhaes, A. L. Weir, B. J. Conrath, P. J. Gierasch, S. S. Leroy, *Nature* 337, 444 (1989); *Icarus* 88, 39 (1990). Theoretical arguments have been presented by U. Lee, T. E. Strohmayer, and H. M. Van Horn [*Astrophys. J.* 397, 674 (1992)].
 22. We thank P. Drossart and B. Bezard for a critical reading of the manuscript. We also thank R. F. Beebe for sending us a video with a movie of polar features as seen by Voyager 1 and 2.

30 November 1992; accepted 9 February 1993

In-Plane Structure of the Liquid-Vapor Interface of an Alloy: A Grazing Incidence X-ray Diffraction Study of Bismuth:Gallium

Erik B. Flom, Mengyang Li, Anibal Acero, Nissan Maskil,*
Stuart A. Rice†

The liquid-vapor interface of a bismuth-gallium mixture (0.2 percent bismuth and 99.8 percent gallium) at 36°C has been studied by grazing incidence x-ray diffraction. The data show, in agreement with thermodynamic arguments, that bismuth is heavily concentrated in the liquid-vapor interface. The x-ray diffraction data are interpreted with the assistance of a simple model that represents the interface as a partial monolayer of bismuth. This analysis leads to the conclusion that the bismuth concentration in the interface is about 80 percent, that there is no significant mixing of gallium and bismuth in the interface, and that the structure function of the interfacial bismuth is like that of supercooled bulk liquid bismuth.

The liquid-vapor interface is a region that separates two fluids that have very different densities. As such, it is an interesting vehicle for the study of inhomogeneous fluids. Consider first a pure liquid. A principal goal of the study of inhomogeneous fluids is the determination of the relations between the

anisotropy associated with the density gradient, intermolecular interactions, the longitudinal structure of the liquid (parallel to the density gradient), and the transverse structure of the liquid (perpendicular to the density gradient). A liquid mixture differs from a pure liquid in that the equilibrium concentrations of the components in the homogeneous bulk and in the liquid-vapor interface will, typically, be different; we expect this segregation of components to alter the structure of that interface.

Most investigations of the structure of the liquid-vapor interface have been concerned with the longitudinal density distribution. In a simple dielectric liquid, such as Ar (or water), both theory and experiment agree that along the normal to the liquid-vapor interface the density decreases smoothly, without subsidiary structure, from the liquid density to the vapor density (1). On the other hand, for a liquid metal, theory predicts (2, 3) and experiment very weakly confirms (4, 5) that the longitudinal density distribution in the liquid-vapor interface has oscillations with a period of an atomic diameter, extending about three atomic diameters into the bulk. For a simple dielectric liquid mixture, theory predicts that the longitudinal density distribution of the component that is in excess in the liquid-vapor interface falls smoothly with distance into the bulk, the range of the decay being several atomic diameters. In contrast, in a liquid metal mixture, such as Cs:Na, theory predicts that the component that concentrates in the liquid-vapor interface forms a nearly pure monolayer, that the immediately adjacent liquid on the bulk side of the interface is depleted in the surface-active component for about an atomic diameter, and that (very nearly) the bulk concentration is reached at a distance of about two atomic diameters into the bulk (3).

Although it has been studied even less than the longitudinal density distribution, the transverse structure of the liquid-vapor interface has been the subject of a number of theoretical and experimental studies. Consider first liquid metals. It has been shown, both experimentally (6, 7) and theoretically (8), that the transverse structure function of the liquid-vapor interface of a pure metal is very similar to the bulk structure function despite the oscillatory nature of the longitudinal density distribution in the liquid-vapor interface. The near identity of the transverse structure function in the liquid metal-vapor interface and the bulk liquid metal structure function characterize a situation very different from that found in crystalline media. In the latter case the surface of the crystal is usually reconstructed and has a different atomic arrangement than does the bulk crystal. On the other hand, when applied to a simple dielectric liquid, the theoretical approach used to describe the liquid metal-vapor interface leads to the prediction that the transverse structure function in the liquid-vapor interface will be different from the bulk liquid structure function. There are, as yet, no experimental tests of this prediction.

This report describes the results of a study of the transverse structure function of the liquid-vapor interface of a Bi:Ga alloy with a bulk composition of 0.2% Bi and 99.8% Ga. In this system the Bi which

Department of Chemistry and the James Franck Institute, University of Chicago, Chicago, IL 60637.

*Present address: Department of Physics, Bar Ilan University, Ramat Gan, Israel.

†To whom correspondence should be addressed.